# Table of Contents



| Updated | Approved |
| --- | --- |
| Specialist Committee on Ice of the 27th ITTC | 27th ITTC 2014 |
| Date 02/2014 | Date 09/2014 |

# Test Methods for Model Ice Properties

## 1. PURPOSE OF THE PROCEDURE

### 1.1 General

The purpose of this procedure is to ensure consistency and comparability of measurements, made in different facilities.

### 1.2 Structure of the Procedure

The sections of this procedure contain a description of acceptable test methods and procedures, the test analyses, a general discussion, including method specific limitations, and quantities to be reported. Most ice properties can be determined by several different methods. The discussion on limitations clarifies which method is most appropriate for specific situations.

### 1.3 General Considerations

In ice testing, Froude's scaling laws are followed. Model testing facilities are using different types of model-ice materials. None of the existing model-ice materials is known to scale all aspects of natural ice. The effect of the geometry of the test specimen on all ice property measurements must be taken into account. In most cases, the values measured are only "indices". However, whether it is an index value or a fundamental mechanical property, the measurement procedure is to be standardized. Many measurements of the past decades refer to the standards stated here and in previous ITTC guidelines.

Model-ice materials are quite weak and environment dependent. To maintain good, reliable results, it is recommended that property measurements are performed in-situ in the tank water whenever possible, without lifting the samples out of the natural environment. The timing and location of the measurements are important. The measurements are to be completed as close as possible to the actual test area and test time.

All measurement procedures are to be very simple, the procedures are to be documented, and the personnel performing the measurements have to be qualified. In all measurements, equipment are to be calibrated in ambient temperatures.

The planning of ice model tests is strongly dependent on the model-ice properties and their ability to scale with respect to the modelled full-scale scenario.

### 1.3 Parameters

| Parameter | Symbol | SI-Units |
|---|---|---|
| Cross-sectional area | $A$ | [m²] |
| Strain modulus of elasticity | $E$ | [Pa] |
| Impact diameter | $D$ | [m] |
| Loading force | $F$ | [N] |
| Buoyancy force | $F_b$ | [N] |

| | | |
|---|---|---|
| Normal loading force | $F_n$ | [N] |
| Tangential loading force | $F_t$ | [N] |
| Bending Moment | $M$ | [Nm] |
| Displaced volume | $V_d$ | [m$^3$] |
| Ice volume | $V_i$ | [m$^3$] |
| Rubble volume | $V_r$ | [m$^3$] |
| Total volume | $V_t$ | [m$^3$] |
| Void volume | $V_v$ | [m$^3$] |
| Section Modulus | $W$ | [m$^3$] |
| Beam, specimen width | $b$ | [m] |
| Dynamic friction coefficient | $c_{if}$ | [m] |
| Ice thickness | $h$ | [m] |
| Foundation factor | $k$ | [kg/m$^2$s$^2$] |
| Gravitational acceleration | $g$ | [m/s$^2$] |
| Beam, specimen length | $l$ | [m] |
| Characteristic length | $l_c$ | [m] |
| Distance from loading point to crack | $l_b$ | [m] |
| Ridge porosity | $p$ | [1] |
| Cross-head speed | $v_c$ | [m/s] |
| Specimen width | $w$ | [m] |
| Displacement | $\delta$ | [m] |
| Poisson's ratio | $\nu$ | [1] |
| Compressive strength | $\sigma_c$ | [Pa] |
| Indentation strength | $\sigma_i$ | [Pa] |
| Flexural strength | $\sigma_f$ | [Pa] |
| Shear strength | $\sigma_s$ | [Pa] |
| Ice density | $\rho_i$ | [kg/m$^3$] |
| Water density | $\rho_w$ | [kg/m$^3$] |

## 2. FLEXURAL STRENGTH OF ICE

### 2.1 General

The flexural strength test should be conducted with specimens from representative locations. At least a set of three samples is to be tested per location to account for natural scatter in results. The location of the samples, in relation to the later test, may be facility specific. In long basins the tests might be conducted a certain distance from both sides of the later test track, whereas in other basins it might be even in the centre of the later test track.

### 2.2 Cantilever Beam Tests

The in-situ cantilever beam test is the most common and best-known method to determine the flexural strength of an ice sheet. A floating cantilever beam having length *l*, and width *b*, is cut in-situ. The tip of the beam is loaded at a constant speed until the beam fails. The loading direction can be either downward or upward, and will correspond to the same bending direction as anticipated in the scheduled model test.

The recommended dimensions of a beam are: $l$ = (5-7)×$h$, $b$ = (2-3)×$h$, where $h$ is the thickness of ice.

Figure 1 reflects the limiting beam dimensions, ensuring that the tested specimen behaves as a beam and not as a plate.

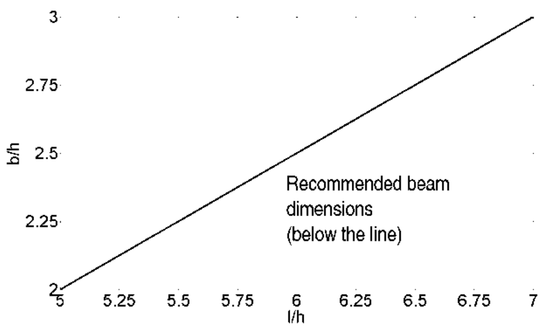


Figure 1: Limiting beam dimension

In order to cut the beams in the same manner each time, it is recommended to use standard patterns/jigs for a selection of ice thickness values. The model-ice should fail in the same mode as in the subsequent mod-tests (mostly brittle, at a higher test speed), but at the same time the speed must be slow enough to avoid significant hydrodynamic effects or specimen damage due to the high local impact of the test plunger. The loading speed (i.e. the displacement rate at the tip) must fulfil the requirements on the brittle failure process. According to Timco (1981) the time-interval between loading and failure should be about 1s-2s. Figure 2 shows an example of the test setup.

The flexural strength, $\sigma_f$, is calculated from Equation 1 following Bernoulli-beam theory (Timco 1981) and Figure 3 shows a sketch of the corresponding beam variables.

$$\sigma_f = \frac{M}{W} = \frac{6Fl_b}{bh^2} \qquad (1)$$

where:

$F$= loading force (measured)

$l$ = beam length (root to tip)

$l_b$= distance from crack location to loading point (ideally equal $l$)

$b$= width of beam

$h$= ice thickness

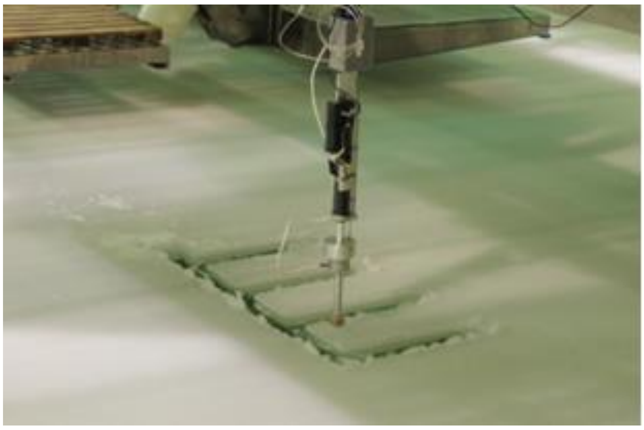

Figure 2: Setup of in-situ cantilever beam test

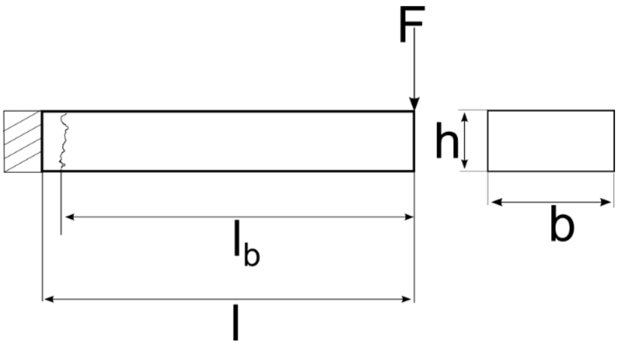


Figure 3: Beam dimensions

## 2.3 Three-Point Bending

The test may be conducted in-situ or ex-situ. The testing-procedure is the same for in-situ and ex-situ tests. In ex-situ testing the beam must be carefully extracted from the ice sheet to avoid any damaging or constitutional changes prior to testing. The test apparatus should consist of round supports to avoid stress concentrations at edges. The beam dimensions should be aligned to the dimensions in Section 2.2, whereas l is here the beam length between the supports. Figure 4 shows a sample test setup, with free supports at both ends. In in-situ tests, it may be more convenient to locate the supports on the top of the beam, while the force is acting from below.

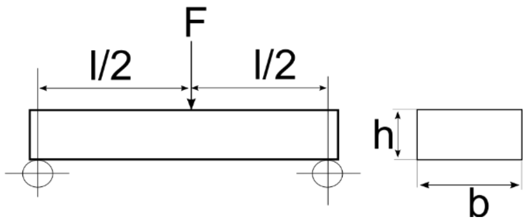


Figure 4: Three point beam bending

The supports must be line supports (point supports in 2D) and should be round. The diameter must be small enough to be a line load and large enough to avoid stress concentrations or notch effects on the ice sample. Equation 2 shows the corresponding formulation to calculate the maximum flexural stress.

$$\sigma_f = \frac{M}{W} = \frac{3Fl}{2bh^2} \tag{2}$$

## 2.4 Limitations and Discussion of the Testing Methods

The parameters obtained from the tests are indices rather than true physical values. This is related to uncertainties and simplifications, which are discussed in the following:

### 2.4.1 Material Constitution

The calculation of the flexural strengths is based on the assumption of homogeneity and an even stress distribution over the cross-section. However, inclusions of air and other local flaws act as stress triggers, which are not accounted for. Additionally, water may drain out when ex-situ tests are conducted. This changes the constitution compared with in-situ tests (see von Bock und Polach et. al (2013)).

The assumed even stress-distribution is additionally based on the assumption of a homogeneous material where the neutral axis of stress is located in the centre of the ice sheet at h/2. FG ice has a quite homogeneous structure over the thickness, whereas columnar ice consists of two layers with often-varying properties. Since the ice model tests are conducted in-situ it is recommended to conduct also the flexural strength tests in-situ.

### 2.4.2 Boundary Conditions

The flexural strength tests are affected by the boundary conditions and their simplifications in Equation 1.

Those are:

Notch effects at the root: This effect is described in Svec et al. (1985) and the size of the radius between ice sheet and beam affects the flexural strength measurement strongly. A decreasing radius increases the notch effect. However, due to practical limitation of the beam length the radius cannot be very large and is usually the size of the mill which is used to cut the beam shape into the ice.

The rigid clamp-support at the root: This is a simplification, and especially here the true mechanical model should account for the vertical and the rotational displacement (see von Bock und Polach, 2005). However, the spring stiffness required for the model is unknown, and hence the modelling with of a rigid clamp is recommended.

Buoyancy effects: The measured net force of the flexural strength test is a superposition of the reaction force due to the response of the model-ice and the buoyancy force due to the submersion of the beam. The buoyancy force is a function of the bending line, which cannot be determined with the generic test setups. Furthermore, for thin ice and small displacements, the buoyancy force may be negligible, and for thicker ice, in some cases, the residual buoyancy force is accounted for, which is, however, an overestimation of this effect.

General: The risk of damaging the test sample or causing constitutional changes is considered very high in the tree-point bending test, and hence, the in-situ cantilever beam test is recommended. When testing the flexural strength of consolidated ridged ice for which in-situ cantilever beam testing becomes impractical, the three-point bending test can be considered an alternative.

### 2.5 Quantities to be reported

- Dimensions of the beam; *l*, *b*, and *h*.
- Failure load; *F*.
- Flexural strength
- (Time-load/deflection curves)
- Date and time of day and location in the basin.

## 3. THE STRAIN MODULUS OF ELASTICITY

The static strain modulus of elasticity is determined by elastic strain measurements, which are usually conducted in model test basins.

### 3.1 Infinite Plate on Elastic Foundation

#### 3.1.1 Infinite Plate-Bending Method A

The infinite plate test is recommended for defining the elastic strain-modulus of model-ice. A model-ice sheet is loaded uniformly over a circular area by placing dead weights in discrete increments. The deflection at the centre of the load is measured by a displacement measuring device. The occurring deflections are very small and the measurement devices must have appropriate sensitivities. The loads should be as small as possible to avoid any plastic deformation of the ice sheet. The load must be applied in the same location where the deflection is measured. In addition, the loads should not remain on the ice sheet long enough to cause large creep deformation in the ice sheet. The load should be applied at a distance of at least four characteristic lengths of the ice sheet from the tank walls. The tank water must be still and sources of vibration (slamming doors etc.) are to be eliminated. The strain-modulus of elasticity is calculated using Equation 3:

$$E = \frac{3}{16}\frac{1-\nu^2}{kh^2}\left(\frac{F}{\delta}\right)^2 \qquad (3)$$

where:

$F$ = loading force,

$g$ = gravitational acceleration,

$k$ = foundation factor ($k = g\ \rho_w$),

$h$ = ice thickness,

$\delta$ = displacement measured,

$\nu$ = Poisson ratio,

$\rho_w$ = water density,

The Poisson's ratio is usually not measured separately, and values of ~0.3 are recommended, see Timco (1981) and von Bock und Polach et al. (2013).

3.1.2 Infinite Plate-Bending Method B

The application of the load and the measurement of the ice sheet deflection in the same location may lead to practical problems. If the displacement is measured in a different loaction than the load, the elastic-strain modulus may be derived numerically by using Bessel functions, (see Chapter 8 in Timoshenko & Woinowsky-Krieger (1959)). This approach delivers the same results as Equation 3.

3.1.3 Infinite Plate-Bending Method C with Larger Load Radius

Sohdi et al. (1982) and later Kato et al. (1999) introduced a procedure for large load radii to determining the static strain modulus of elasticity from plate bending experiments by using the characteristic length, $l_c$:

$$l_c^2 = \frac{\Delta F}{\Delta \delta}\frac{1}{8k}Z \quad (4)$$

$$Z = 1 + \frac{\alpha^2}{2\pi}\left(\ln\frac{\gamma\alpha}{2} - 5/4\right) \quad (5)$$

where $k$ is the specific weight of water, r is the radius, $\alpha = r/l_c$ and $\ln \gamma = 0.5772$ (Euler's constant). It should be noted that Z is approximately equal to 1.0 for low values of $\alpha$ (<0.2). The elastic modulus, E, of a model-ice sheet is then obtained from Equation 7:

$$l_c = \sqrt{\frac{Eh^3}{12(1-\nu^2)k}} \quad (6)$$

$$E = \frac{12(1-\nu^2)kl_c^4}{h^3} \quad (7)$$

where:

$l_c$ = characteristic length.

All other parameters are the same as in Section 3.2.1

## 3.2 Beam Bending Tests

The elastic strain modulus can be determined by cantilever beam tests and the use of the beam-bending differential equation. Such measurements can be combined with the flexural strength measurements. The beam displacement must be determined at five locations to interpolate the beam bending line and to provide sufficient boundary conditions to determine the unknowns. The method is based on the beam bending differential equations (see von Bock und Polach, 2005). Furthermore, the impact of the elastic foundation is not taken into account.

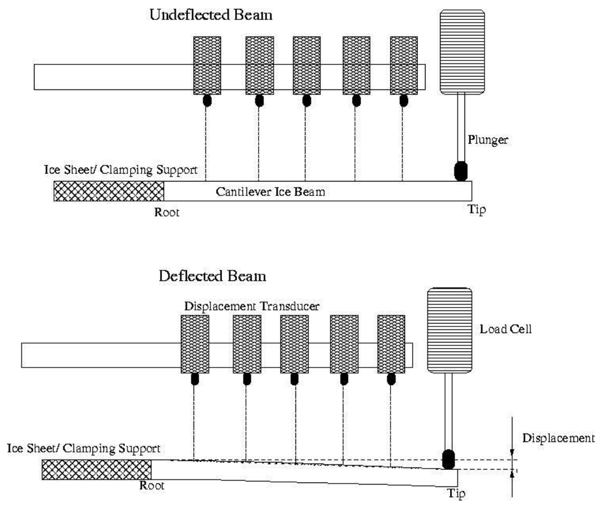


Figure 5: Test setup for determining elastic strain modulus based on beam bending tests (von Bock und Polach, 2005)

More details on the procedure are found in von Bock und Polach (2005).

## 3.3 Limitations and Discussion of the Testing Methods

It must be acknowledged that for the plate deflection method the measured displacements might be very small. This does not only require a high resolution displacement transducer (in most cases a laser), but also a vibration free mounting point. Already small oscillation amplitudes may disturb the measurements too much.

The theory used for the plate on elastic foundation is based on thin plate theory and plain stress. As shown in von Bock und Polach et al. (2013) neglecting shear stresses may lead to an error. This error may increase for increasing thickness. Therefore, this parameter should be considered as an index. Furthermore, Frederking and Timco (1983) examined various influence factors on the elastic strain modulus measurements by beam bending tests.

It must be considered that the plate bending method Option A and B assume a point-load, whereas Option C accounts for larger load radii (parameter $r / \alpha$ in Equation 5). The combined flexural strength and strain modulus test faces practical challenges. Especially in thin ice, the beams are short and it may be difficult to fit all displacement transducers onto the setup. The beam test is the most common test used in full scale.

The beam bending method is difficult to handle in practice and the high number of measured parameters (five displacement measurements) may lead to a significant error accumulation. Furthermore, the plate-bending test is the most common test method and therefore recommended to use.

## 3.4 Quantities to be Reported

### 3.4.1 Infinite Plate on Elastic Foundation

- Thickness of model-ice sheet
- Weights used
- Location in the tank
- Time-deflection curves
- Calculated modulus of elasticity
- Time of the day when measured

### 3.4.2 Beam Bending Method

- Thickness of model-ice sheet
- Measured bending force
- Location of displacement transducers
- Interpolated bending line
- Location in tank
- Time-deflection curves
- Calculated modulus of elasticity
- Time of day when measured

# 4. MODEL-ICE DENSITY

## 4.1 Measurement Approaches

Density / specific weight measurements are recommended to be completed ex-situ to raise the precision in measurements and results. The test may be conducted with two similar approaches. Figure 7 shows the test setup. The ice piece is submerged in a container and the water displaced due to submerging is drained out, collected and weighed (Option A). During the process the submerging force is measured with a load-cell, which is located above the tripod in Figure 6.

Figure 6: Ex-situ density measurement setup (Option A)

The density of ice is calculated using the following Equation 8, where $V_d$ is the volume of the displaced water (equal to the submerged ice volume) and $F$ the (buoyancy-) response force of the submerged ice piece.

$$\rho_i = \rho_w - \frac{F}{V_d g} \qquad (8)$$

Figure 7 presents a variation of the ex-situ density measurement (Option B). The water is not drained, but the surface elevation of the water level is measured with a laser that is pointing at a floater which position vertically changes once the ice is submerged.

The density measurements Option A and B may be simplified by determining the displaced volume with a calliper of measurement tape. However, the accuracy of this method may not in all cases be good enough.

Another way of measuring the density is Option C presented in Figure 8 and Figure 9. Here, only submerging weight (Figure 9) needs to be measured and the ice density may be calculated according to Equation (9). The measurement should be conducted on a level surface.

$$\frac{\rho_i}{\rho_w} = \frac{w_2 - w_1}{w_3 - w_1} \qquad (9)$$

Figure 7: Ex-situ density measurement setup (Option B)

Figure 8: Force balance measurement without displacement recording (Option C)

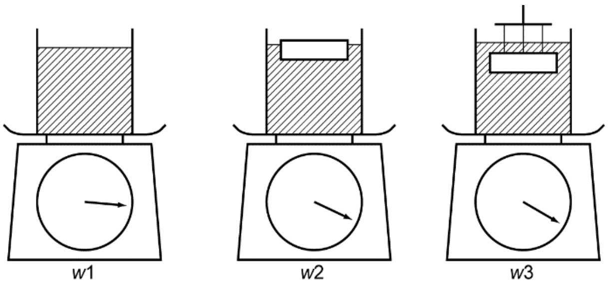


Figure 9: Steps of density measurement (Option C)

## 4.2 Limitations and Discussion of the Testing Methods

The in-situ measurements have the advantage that the ice does not need to be extracted and fluids are not draining out. Therefore, it is recommended to float the ice piece over the measurement container and extract ice and water together. The ex-situ measurements have been developed whereby the displaced water can be determined with higher accuracy. Here, extracting the model-ice piece physically should be avoided. Instead, the piece should be floated over the submerged container and extracted together with tank water. Option A is found to be problematic for thinner ice, because the amount of drained water is small and some of it is found to remain in the drain (drops). Additionally, the process might be time consuming. Option B is found suitable to overcome the draining problem and to measure the surface elevation with high accuracy. Nevertheless, the handling of the ice pieces in ex-situ testing can be difficult, especially for thin ice.

Option C is very straightforward, but requires a scale with a high sensitivity and a level working surface. The advantage of option C is that only the weight needs to be measured.

### 4.3 Quantities to be Reported

- Volume of ice piece tested
- Measured submergence load
- Specific weight of the tank water
- Calculated specific weight of the model-ice

## 5. COMPRESSIVE STRENGTH OF ICE

### 5.1 Uniaxial Compression Tests

The compressive strength of model-ice is important, especially for the horizontal loading direction, when ice impacts rigid vertical structures it may fail in compression. The compressive strength of model-ice can be defined by in-situ or ex-situ tests. As for the other testing methods, it is recommended to conduct in-situ test to assure structural integrity and to avoid constitutional changes.

In-situ tests may be conducted by cutting out a specimen as a cantilever beam while pushing / compressing it from the free end side (see Figure 12). In ex-situ tests, the specimen may be located between two steel plates to compress it (see Figure 10 and Figure 11). Compressible material (urethane polyester see Figure 8) is placed between the compliant platens and the ice to compensate relative unevenness. Ice samples are carefully prepared by a milling machine or surface grinder and placed in between the two loading plates of the test frame. Compliant platens, or a thin sheet of other compressible materials (e.g. paper), are used in order to avoid sliding of the specimen and to apply a uniform axial load. In both cases the compressive stress is determined by Equation 10.

$$\sigma_c = \frac{F}{A} \qquad (10)$$

where:

$F$ = failure force

$A$ = width * ice thickness

Recommended Dimensions:
Beam length = 4 * ice thickness
Beam width = 2 * ice thickness

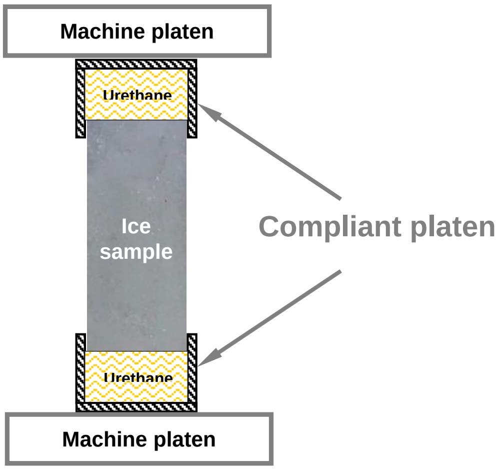


Figure 10: Compressive ex-situ test principle

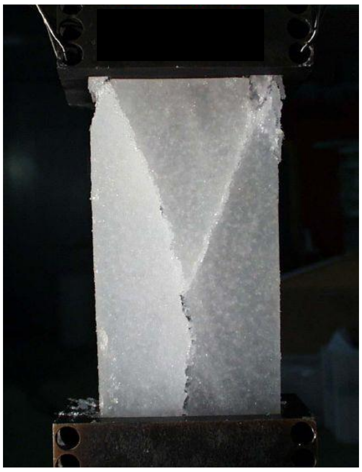

Figure 11: Compressive ex-situ test setup

Alternative dimensions:

Beam length = ice thickness

Beam width = ice thickness

Crosshead speed = sufficiently high to cause brittle failure (in all cases) or according to Equation (11)

$$v_c = v_{ice} \frac{l}{4w} \quad (11)$$

where:

$v_c$ = rate of feed

$v_{ice}$ = ice drift velocity

$l$ = sample length (= 4 x ice thickness)

$w$ = structure width

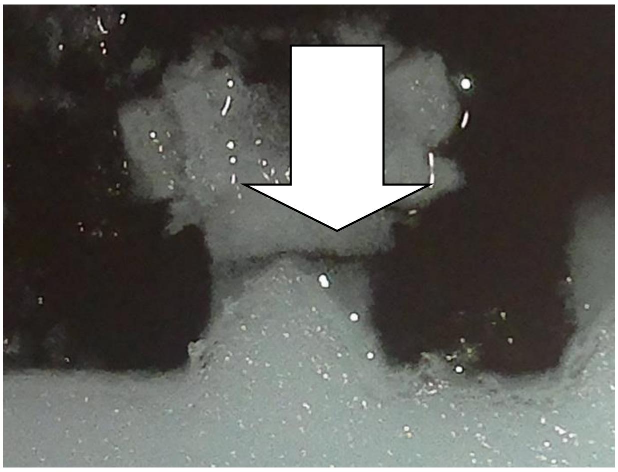

Figure 12: Compressive in-situ test with compressed cubic specimen and indicated loading direction

## 5.2 Quantities to be reported

- Dimensions of the indenter
- Ice thickness tested
- Location of the tests in the tank
- Time of measurements
- Speeds
- Measured loads
- Calculated compressive strength

## 5.3 Limitations and Discussion of the Testing Methods

It must be acknowledged that in the compressive test and the measured failure load depends heavily on the specimen dimensions. Therefore, the maintenance of the geometry is very important. Two different geometries are stated to account for the different geometries used in the past. Larger specimens ease the handling in ex-situ testing, while smaller specimens have a higher stiffness than more slender specimens do. The higher stiffness is advantageous when impact surface and specimen surface are not exactly parallel. In this case, the crushing and shearing may occur in the contact interface until the two surfaces are parallel and the actual compression starts. Accordingly, more slender specimens may fail by a superposition of compression and other failure modes, such as buckling or bending. Therefore, it is recommended to compensate for unparallel faces with soft and compressible material in between.

### 5.4 Quantities to be Reported

- Measured load, *F*
- Test specimen dimension
- Test setup
- Compressive strength
- Photographs of failed specimens, if possible

## 6. INDENTER TEST

The indenter test determines the force related to ice failing by crushing on a round structure. A possible test setup is illustrated in Figure 13. The indenter test is in-situ measurements, which eliminates the effect of possible changes of ice properties caused by moving the ice sample. Other than in the test shown in Figure 12 the test area is confined by the surrounding ice sheet, which enforces the failure by crushing. In the indenter test a cylinder with a force sensor is pushed through the ice sheet with constant velocity in the brittle range (1 mm/s – 10 mm/s advance speed). The measurement is usually repeated with different velocities, to assure speed independent results. The diameter of indenter *D* is chosen in dependency on the ice thickness *h*, so that the ration $D/h > 1$.

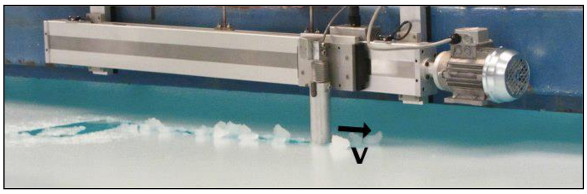


Figure 13: Measurement of crushing strength using the indenter test. A cylinder with a force sensor is pushed through the ice sheet with a constant velocity.

The crushing strength based on the indentor method is determined, according to Korzhavin (1962)

$$\sigma_i = \frac{F}{ci \cdot mDkh} \tag{12}$$

where

$F$ = force (measured)

$m$ = shape factor (round structure 0.9)

$k$ = contact factor (0.4 - 0.7)

$h$ = ice thickness

$D$ = diameter of indenter

$ci$ = factor depending on the D/h ratio

The contact factor $k$ takes into account the incomplete contact between ice and indenter. In case of brittle breaking phenomenon, the factor $k$ is 0.4 and in case of ductile breaking the factor is 0.7.

The parameter ci is determined from

$$ci = \sqrt{1 + 5\frac{h}{D}} \tag{13}$$

## 7. SHEAR STRENGTH

### 7.1 Punch Through Test

A 200 mm x 300 mm piece of ice is removed from an ice sheet and a 35 mm diameter hole is punched through it. One data point is the mean of five or six samples. The shear strength is determined according to

$$\sigma_S = \frac{F}{D\pi\, h} \tag{14}$$

where:

$h$ = ice thickness

$F$ = load

$D$ = punch diameter

## 8. ICE- MODEL FRICTION COEFFICIENT

The ice friction coefficient is a dimensionless parameter, and, according to Froude- scaling, the dynamic friction coefficient is to be the same in model-scale as in full scale. Friction is a lubricant phenomenon which varies with temperature, contact pressure, and also slightly with the relative velocity between the ice and substrate material. The friction coefficient may be determined on two ways. One is the physical ice-model friction test, and another one is based on surface roughness tests.

### 8.1 Physical Ice-Model Friction Coefficient

It is recommended to determine the friction coefficient by towing a block of ice over the material surface (wet or dry depending on the test conditions). It is important that this surface be perfectly horizontal. The ice and material surface should be described. The initial peak resistance divided by the normal force represents the static friction coefficient (Schwarz et al., 1981).

Prior to the tests, the ice sample weight must be determined. The ice-specimen is then moved with constant speed over the test surface, while the horizontal force is measured. Depending on the ice sample constitution, it may be possible to increase the vertical load with a board and deadweights loaded on top. Care must be taken to ensure the ice is not compressed too much.

A testing apparatus should be used to determine the dynamic ice-friction coefficient. During the coating process of the model a plate with the same surface characteristics is manufactured for the fiction test. Alternatively, the test may be conducted on the model directly (bottom surface).

The tests may be conducted with a wetted surface or a dry surface, which must be mentioned explicitly. It is recommended to use a wet friction surface, as this is also encountered by the ship models.

$$c_{\mathrm{if}} = \frac{F_{\mathrm{t}}}{F_{\mathrm{n}}} \tag{15}$$

$C_{\mathrm{if}}$ = dynamic friction coefficient

$F_{\mathrm{t}}$ = mean value of measured tangential force

$F_{\mathrm{n}}$ = normal load

### 8.2 Surface Roughness Related Friction

The relation of surface roughness and friction coefficient can only be established by tests as described in 7.1 and simultaneous surface roughness measurements. The curve-fitting requires at least 5 samples whereas two have to reflect the extremes, very rough and very smooth. Subsequently it suffices to measure the surface roughness on the model to determine the friction coefficient. However, it is desirable to conduct as many friction experiments and surface roughness measurements simultaneously as possible to improve the curve fitting and the knowledge on impact factors such as temperature etc.

### 8.3 Limitations and Discussion of the Testing Methods

The friction tests described can be conducted on long boards that are painted together with the model or on the model. The long boards have the advantage of a long testing distance, while the test directly on the model has a rather short test length. Additionally it may not be feasible to conduct the tests on the model due to a too curvy hull shape. However, the surface roughness may even vary over the model surface area and also the painting of a separate board might lead to surface differences compared to the model hull.

### 8.4 Quantities to be Reported

- Horizontal towing forces, $F_t$
- Total normal force, $F_n$
- Dimensions of the ice block (length, width and thickness)
- Sample weight (prior to test)
- Rear weight
- Velocity
- Ice specimen temperature
- Wet or dry friction test
- Upper or bottom side of the ice
- Description of the test setup

## 9. ICE THICKNESS MEASUREMENTS

The thickness measurements of model-ice may be combined with any of the strength measurements. The accuracy of the measurement must be high enough to determine the thickness with an accuracy of ~1mm (at least). While conducting the measurements the ice must be handled with utmost care to avoid sample damages, e.g. compressing the ice with the calliper (see Figure 14) that may falsify the measurement.

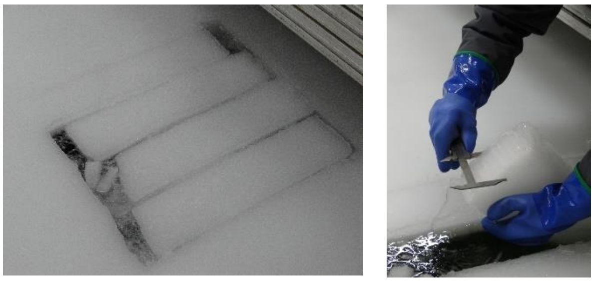

Figure 14: Ice thickness measurements with calliper

The ice thickness should be measured in 1m-2m space intervals along the broken channel. It must be noted that in propulsion tests the propeller wake might affect the model ice thickness. In the event that a broken channel is not available for ice thickness measurements a comparable set of thickness measurements must be obtained to develop a representative ice thickness distribution.

## 10. RIDGE TESTS

### 10.1 Ice Ridges and Ice-rubble

After the ridge has been built, the keel depth and sail height are determined by profiling. In general, three profiles are taken, preferably in the area of the model trace (portside – centre – starboard). This may be achieved by pressing a stick in equidistant intervals through the ridge.

At the lower end of the stick a cross-bar is activated and the, stick can be lifted upwards until a certain resistance indicates the bottom of the ridge. The keel depth is then read from a scale, (see e.g. Figure 17).

Alternatively, the underwater contours of the ridge can be profiled with an acoustic echo sounder, and the sail topography above water by laser level (Sutherland, J. & Evers, K.-U. ,2012).

Figure 15 Ridge-profiling device to determine keel depth and sail height

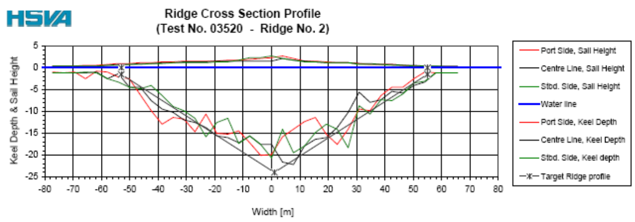


Figure 16 Cross section profiles of an ice ridge

### 10.1.1 Quantities to be reported

- Time of measurement
- Sail height and width
- Keel depth and width
- Thickness of consolidated layer

## 10.2 Shear strength of ice-rubble

Ice-rubble in a ridge is usually considered as a bunch of ice pieces without cohesion. A wide scatter of values for the angle of internal friction (φ) has been reported. A plug or a pushdown test where the consolidated layer is pre-cut and the rubble is loaded vertically was originally completed in-situ by Leppäranta and Hakala (1992), and has been completed in the laboratory by Azarnejad and Brown (1998). One problem is the derivation of material properties from the recorded force and displacement, as the stresses on the failure plane are not known (Jensen et al. 2000).

### 10.2.1 Punch Test

In model scale, the internal shear strength of an unconsolidated ridge is determined by a so called "punch test". This test should be conducted immediately after the model has passed the ice ridge. If possible, the test site of the punch test should be a sufficient distance from the track of the model and the ice tank walls.

Where the keel ice-rubble is covered by a ''consolidated layer'' a circular trench is cut through this layer about 1 cm to 2 cm beyond the punching cylinder. It is important to cut only through the consolidated layer and not into the rubble ice pieces below in order to keep the ridge fragments as stable as possible. The ridge depth should be measured clockwise at least eight times on a circle about 5 cm beyond the edge of the punching cylinder. The device for punch tests consists of a heavy steel cylinder (~300kg). The lowering speed should be sufficiently high to avoid disturbances of the ridge structure and sufficiently low to avoid hydrodynamic effects (good experience is made with 7 mm/s). The load is measured with a load cell between cylinder and crane hook. (see Figure 17).

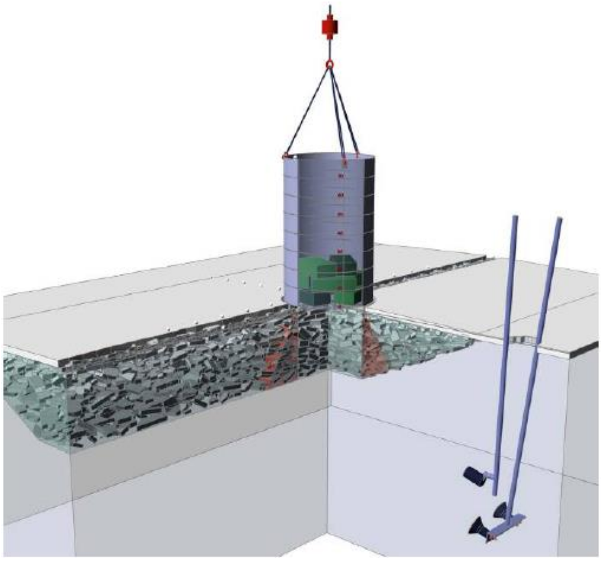

Figure 17 Circular cylinder with ballast weights is lowered down on the ridge

10.2.2 Open Water Test

Since the punching procedure is also affected by the buoyancy of the submerging cylinder with ballast weights, tests in open water must be carried out. The punching cylinder including the ballast weights is lowered into the ice-free water with the same lowering speed as in the ridge punch tests.

For low speed (v ~ 7 mm/s) it can be assumed that the change in the measured force is mainly related to the buoyancy of the cylinder and ballast weights being submerged.

10.2.3 Test Analysis

In order to derive the pure shear force generated by the ice-rubble, the forces measured in the open water test must be subtracted from the forces measured in the ridge punch tests. In a second step the buoyancy force of the ice-rubble below the cylinder must be determined (after the cylinder has been stopped at the lowest position) and also subtracted. Assuming that the shear force is acting along a cylindrical surface (instead of a slightly conical surface) which linearly decreases with the immersion depth of the cylinder, the stress in the shear plane can be calculated.

## 10.3 Ridge / rubble porosity

The porosity, p, of an ice accumulation is determined by estimating the volume of ice contributing to the ice accumulation, from

$$p = \frac{V_v}{V_t} = 1 - \frac{V_I}{V_t} \tag{16}$$

$V_v$ is the volume of both voids, above and below the water surface, $V_i$ is the volume of the ice, and $V_t$ is the total volume of the rubble. The number of actual porosity field measurements is small. According to White (1999) most reported values are based on estimates or back-calculated based on other ice variables.

In some cases, density *D* of frazil deposits or accumulations has been reported. Density and porosity are related as follows:

$$p = 1 - \frac{D}{\rho_i} \tag{17}$$

For modelling ridges and ice-rubble in ice tank tests the porosity may range from $0.3 < p < 0.4$.

In order to estimate the porosity and macro-density of the ice ridge keel, so-called macro buoyancy tests can be conducted. For these test a translucent cylinder closed only at the top is submerged into the ridge. The cylinder is connected to a crane with a load cell in between. The signal of the load cell indicates the buoyancy force caused by the ice-rubble. The rubble volume inside the cylinder can be estimated from underwater video screenshots (Figure 18).

Figure 18 Illustration of macro-buoyancy cylinder penetrated through ridge (left), submerged translucent cylinder filled with ice-rubble (right)

The macro density of ice-rubble can be calculated by

$$\rho_{\mathrm{r}} = \frac{V_{\mathrm{r}}\rho_{\mathrm{w}} g F_B}{V_{\mathrm{r}} g} \qquad (18)$$

where

$\rho_r$ = macro-density of ice-rubble

$\rho_W$ = water density

$V_r$ = rubble volume in cylinder

$F_B$ = measured buoyancy force

$g$ = gravity constant

The macro porosity can be calculated by Equation 19.

$$\eta = \frac{\rho_{\mathrm{r}} - \rho_{\mathrm{i}}}{\rho_{\mathrm{w}} - \rho_{\mathrm{i}}} \qquad (19)$$

where

$\eta$ = macro- porosity of ice-rubble

$\rho_r$ = macro-density of ice-rubble

$\rho_W$ = water density

$\rho_i$ = ice density (level ice)

The macro-buoyancy and macro-porosity tests are rather time consuming and need additional experienced personnel for these kind of tests.

## 11. REFERENCES

Azarnejad A., and Brown T.G. 1998. Observations of ice-rubble behaviour in punch tests, In Proceedings of the 14th International Symposium on Ice (IAHR), Postdam, NY,USA, 589-596

Frederking, R and Timco, G (1983) On measuring flexural properties of ice using cantilever beams, Annals of Glaciology 4

Jensen, A., Hoyland, K. V., Evers, K.-U. 2000. Scaling and measurement of ice-rubble properties in laboratory tests Proceedings of the 15th International Symposium on Ice (IAHR), August 28 - September 1, 2000, Gdansk, Poland, Vol. 1, pp. 105- 112, ISBN 83-85708-39-1

Kato, K., Nixon, W., Jones, S., Wilkmann, G., Izumiyama, K., Sazanov, K., 1999. The specialist committee on ice, final report and recommendations to the 22nd ittc. In: Proc. of the 22 Int. Towing tank conference (ITTC), Seoul, South Korea. pp. 349-373

Korzhavin, K.N., 1962.Action of Ice on Engineering Structures. USSR Acad. Sci Siberian Branch. CRREL Draft Translation No. 260, Hanover, 1971.

Leppäranta, M. and Hakala, R.1992.The structure and strength of first-year ice ridges in the Baltic, Cold Regions Sciences and Technology, 20, pp. 295-311

Schwarz, J., Frederking, R., Gavrillo, V., Petrov, I.G., Hirayama, K.-I., Mellor, M., Tryde, P.and Vaudrey., K.D. 1981. Standardized Testing Methods for Measuring Mechanical Properties of Ice – Prepared by the Working Group on Standardizing Testing Methods in Ice, IAHR Section on Ice Problems, Cold Regions Science and Technology, 4 (1981) 245-253

Sodhi, D.S., K. Kato, F.D. Haynes and K. Hirayama, 1982. Determining the characteristic length of model ice sheets. Cold Regions Science and Technology, vol. 6, pp. 99-104

Sutherland, J. & Evers, K.-U. (Eds.). 2012. Foresight study on laboratory modelling of wave or ice loads on coastal and marine structures. Report of the Hydralab Consortium, EC contract no. 261520, HYDRALAB-IV, Deliverable D2.3

Svec, O., Thompson, J., & Frederking, R. (1985). Stress concentrations in the root of an ice cover cantilever: Model tests and theory. Cold Regions Science and Technology .

Timco, G. (1981). On the test methods for model-ice. Cold Regions Science and Technology. Vol. 4 pp. 269-274

Timoshenko, S., & Woinowsky-Krieger, S. (1959). Theory of Plates and Shells. McGraw-Hill.

von Bock und Polach, R. F. (2005). Sea ice characteristics and its impact on model tests (master thesis). Berlin: Technical University of Berlin.

von Bock und Polach, R. F., Ehlers, S., & Kujala, P. (2013). Model Scale Ice - Part A: Experiments. Cold Regions Science and Technology .

White, K. D. (1999). Hydraulic and Physical Properties Affecting Ice Jams, CRREL Report 99-11, US Army Corps of Engineers Cold Regions Research & Engineering Laboratory, Hanover NH, USA, December 1999